

In Situ Precision Cell Electrospinning as an Efficient Stem Cell Delivery Approach for Cutaneous Wound Healing

Citation for published version (APA):

Wen, Z., Chen, Y., Liao, P., Wang, F., Zeng, W., Liu, S., Wu, H., Wang, N., Moroni, L., Zhang, M., Duan, Y., & Chen, H. (2023). In Situ Precision Cell Electrospinning as an Efficient Stem Cell Delivery Approach for Cutaneous Wound Healing. *Advanced Healthcare Materials*, 12(26), Article 2300970. <https://doi.org/10.1002/adhm.202300970>

Document status and date:

Published: 01/10/2023

DOI:

[10.1002/adhm.202300970](https://doi.org/10.1002/adhm.202300970)

Document Version:

Publisher's PDF, also known as Version of record

Document license:

Taverne

Please check the document version of this publication:

- A submitted manuscript is the version of the article upon submission and before peer-review. There can be important differences between the submitted version and the official published version of record. People interested in the research are advised to contact the author for the final version of the publication, or visit the DOI to the publisher's website.
- The final author version and the galley proof are versions of the publication after peer review.
- The final published version features the final layout of the paper including the volume, issue and page numbers.

[Link to publication](#)

General rights

Copyright and moral rights for the publications made accessible in the public portal are retained by the authors and/or other copyright owners and it is a condition of accessing publications that users recognise and abide by the legal requirements associated with these rights.

- Users may download and print one copy of any publication from the public portal for the purpose of private study or research.
- You may not further distribute the material or use it for any profit-making activity or commercial gain
- You may freely distribute the URL identifying the publication in the public portal.

If the publication is distributed under the terms of Article 25fa of the Dutch Copyright Act, indicated by the "Taverne" license above, please follow below link for the End User Agreement:

www.umlib.nl/taverne-license

Take down policy

If you believe that this document breaches copyright please contact us at:

repository@maastrichtuniversity.nl

providing details and we will investigate your claim.

In Situ Precision Cell Electrospinning as an Efficient Stem Cell Delivery Approach for Cutaneous Wound Healing

Zhengbo Wen, Yuxin Chen, Peilin Liao, Fengyu Wang, Weiping Zeng, Shoupei Liu, Haibing Wu, Ning Wang, Lorenzo Moroni, Minmin Zhang,* Yuyou Duan,* and Honglin Chen*

Mesenchymal stem cell (MSC) therapies have been brought forward as a promising treatment modality for cutaneous wound healing. However, current approaches for stem cell delivery have many drawbacks, such as lack of targetability and cell loss, leading to poor efficacy of stem cell therapy. To overcome these problems, in the present study, an in situ cell electrospinning system is developed as an attractive approach for stem cell delivery. MSCs have a high cell viability of over 90% even with a high applied voltage of 15 kV post-cell electrospinning process. In addition, cell electrospinning does not show any negative effect on the surface marker expression and differentiation capacity of MSCs. In vivo studies demonstrate that in situ cell electrospinning treatment can promote cutaneous wound healing through direct deposition of bioactive fish gelatin fibers and MSCs onto wound sites, leading to a synergic therapeutic effect. The approach enhances extracellular matrix remodeling by increasing collagen deposition, promotes angiogenesis by increasing the expression of vascular endothelial growth factor (VEGF) and forming small blood vessels, and dramatically reduces the expression of interleukin-6 (IL-6) during wound healing. The use of in situ cell electrospinning system potentially provides a rapid, no touch, personalized treatment for cutaneous wound healing.

a natural capacity for self-regeneration; however, this process is limited in acute and extensive wounds, burns, and elderly and diabetic patients.^[3] Current evidence suggests that around 100 million people require skin wound treatment every year in China,^[4] and this number may continue to grow due to the aging population and increasing incidence of diseases such as obesity and diabetes. Despite autografts being considered as the gold standard treatment for skin regeneration, limitations in donor site availability and complications associated with repeated donor tissue harvesting demand new therapies for skin wound healing.^[5]

In recent years, stem cell therapies, especially mesenchymal stem cells (MSCs), have been broadly investigated in clinical and preclinical trials in wound healing.^[6] MSCs are adult stem cells originating from the mesoderm found in various tissues, including bone marrow, muscle, umbilical cord blood, and endometrium.^[7] There is an increasing consensus suggesting that MSCs have a stimulatory effect on cutaneous

1. Introduction

Skin, body's largest organ, covers the entire body, accounting for approximately 14–16% of body weight.^[1,2] The skin possesses

wound healing and skin regeneration mainly through immune regulation, anti-inflammatory, and vascularization responses.^[8] The remarkable therapeutic potential of MSCs in skin wound healing has resulted in the development of ideal methods for


Z. Wen, Y. Chen, P. Liao, F. Wang, W. Zeng, S. Liu, H. Wu, N. Wang, Y. Duan, H. Chen
Laboratory of Stem Cells and Translational Medicine
School of Medicine
South China University of Technology
Guangzhou 510006, China
E-mail: yuyouduan@scut.edu.cn; chenhl@scut.edu.cn

L. Moroni
MERLN Institute for Technology-Inspired Regenerative Medicine
Complex Tissue Regeneration Department
Maastricht University
Maastricht 6229 ER, The Netherlands

M. Zhang
Guangdong Provincial Key Laboratory of Nanophotonic Functional Materials and Devices
School of Information and Optoelectronic Science and Engineering
South China Normal University
Guangzhou 510006, China
E-mail: zhangminmin@m.scnu.edu.cn

Y. Duan
National Engineering Research Centre for Tissue Restoration and Reconstruction
South China University of Technology
Guangzhou 510006, China

H. Chen
Medical Research Institute
Guangdong Provincial People's Hospital (Guangdong Academy of Medical Sciences)
Southern Medical University
Guangzhou 510080, China

 The ORCID identification number(s) for the author(s) of this article can be found under <https://doi.org/10.1002/adhm.202300970>

DOI: 10.1002/adhm.202300970

delivering MSCs including local injection,^[9] systemic injection,^[10] cell spraying,^[11] and using scaffolds as carriers.^[8,12] Local and systemic injections have disadvantages such as low cell survival rates, poor localization, and tissue targeting. In addition, the injection methods are invasive, which might cause a painful or uneasy feeling in patients. Although cell delivery by spraying represents an attractive topical administration approach, the poor control of cell deposition and limited cell survival numbers are limiting factors. Different scaffolds including electrospun fibrous mesh have been harnessed as carriers for efficient MSC delivery for wound healing. In typical application scenarios, stem cells are seeded onto sterile scaffolds forming cell-scaffold constructs, then cell-scaffold constructs are transplanted to wound sites for skin regeneration. In many cases, cell-scaffold constructs encounter difficulties in achieving optimal alignment with the shape of the wound.

Gelatin is a natural protein polymer that is both biocompatible and biodegradable. It can be obtained from animal collagen through partial hydrolysis and thermal degradation.^[13] Due to its low cost, biocompatibility, safety, non-immunogenicity, and biodegradability, gelatin has been widely used in food, medical, cosmetic, and pharmaceutical products.^[14] Currently, swine and cattle skin and bone account for approximately 98% of the sources of gelatin. However, in recent years, there has been a risk of human infection from animal diseases such as bovine spongiform when consuming mammalian-derived gelatin.^[15] Therefore, gelatin from marine sources was proposed as an alternative. Among these, cold-water fish gelatin has gained much attention as a base material in the biomedical field. Aqueous cold-water fish gelatin can maintain its liquid state at both human body and room temperature, while mammal gelatin easily shifts to a gel state, which makes it difficult to electrospin at human body and room temperature.^[14]

Electrospinning is a technique extensively investigated over the last two decades for wound healing applications.^[16] Recently, in situ electrospinning, which refers to the direct deposition of nanofibers onto wound sites, has gained much attention. Compared with traditional electrospinning methods, in situ electrospinning could produce fibers to better and efficiently match the wound site, especially for the uneven surface of the wound.^[17] Practically, in situ electrospinning could be achieved by employing a portable or handheld electrospinning device that is safe and easy to operate.^[17] Dong et al. conducted a study to test the feasibility of using a handheld electrospinning device for the deposition of poly(*ε*-caprolactone)/Ag-MSNs composite fibers onto wounds in rats.^[18] Their studies demonstrated that these nanofibrous membranes with antibacterial properties could help reduce inflammation and speed up wound healing. Zhao et al. developed a self-powered portable melt electrospinning device that can be used for in situ wound dressing.^[19] To the best of our knowledge, few works on in situ electrospinning produced electrospun fibers with embedded living cells.

In the present study, we hypothesized that in situ cell electrospinning could deliver MSCs to wound sites for cutaneous wound healing. To examine this hypothesis, we initially prepared a spinning solution that contained cold fish gelatin and viable MSCs. The impact of applied voltage during cell electrospinning on MSC viability, cell surface markers, and differentiation capacity was investigated. A model of cutaneous wound healing

(Sprague Dawley (SD) rat) was used to evaluate the therapeutic potential of our cell electrospinning approach for skin wound healing.

2. Results and Discussion

MSCs play an active role in promoting wound healing, and ample literature has substantiated the therapeutic potential of MSCs to improve cutaneous wound healing outcomes.^[20] However, one of the key challenges restricting the effectiveness of MSCs is the mode of cell delivery to damaged tissues.^[9] Herein, we present a contact-free, targeted delivery approach with high cell viability to deliver stem cells to skin wound sites (**Figure 1**). As shown in Figure 1, gelatin aqueous solution was prepared and then mixed with living cells to form a “bioink”. The bioink was loaded onto a portable handheld electrospinning device, enabling the direct deposition of cell-laden fibers onto the skin wound sites.

2.1. Effect of Polymer Solution on Cell Electrospinning

Cold-water fish gelatin was used as a polymer to prepare the electrospinning solution due to two reasons. Cold-water fish gelatin is a water-soluble polymer that can maintain the solution at both the human body and room temperature. As shown in Figure S1 (Supporting Information), porcine gelatin aqueous solution showed signs of gelation at room temperature at a relatively low concentration of 6% (w/v), below the critical entanglement concentration needed for generating electrospun fibers.^[14] As a consequence, porcine gelatin/water systems could not be processed with electrospinning without additional facilities.^[14] Unlike gelatin derived from mammalian, cold-water fish gelatin in an aqueous solution does not gelate at room temperature even at a high polymer concentration of 70% (w/v), making it spinnable at room temperature. The solvent (water) is evaporated during cell electrospinning and gelatin fibers were formed. Another important feature is the bioactive property of cold-water fish gelatin.

Next, we investigated the effect of polymer concentration on fiber morphology. As shown in Figure S2 (Supporting Information) in our revised manuscript, bead-like structure embedded in fibers was observed with a gelatin concentration of 30% (w/v). As the gelatin concentration reaches to 50% and 70% (w/v), homogeneous fibers were obtained. It is worth noting that electrospinning solution of 70% gelatin becomes viscous, which is unfavorable for subsequent mixing with living cells. Therefore, we chose 50% gelatin for further investigation. **Figure 2A** shows the handheld electrospinning apparatus used in our lab. The apparatus was operated by one hand, and the cold-water fish gelatin fibrous membrane can be rapidly spun onto the other hand, indicating the good electrospinning ability of cold-water fish gelatin (Figure 2B,C). Informed consent was given prior to this part of the experiment. The average diameter of fish gelatin fibers was 184 ± 34 nm (Figure 2D). Using a high concentration of fish gelatin enhances the feasibility of electrospinning, and protects MSCs from the damaging effect of high voltage. As shown in Figure S3 (Supporting Information), cell electrospinning with Gelatin/PBS(Phosphate-Buffered Saline)solution yielded a cell

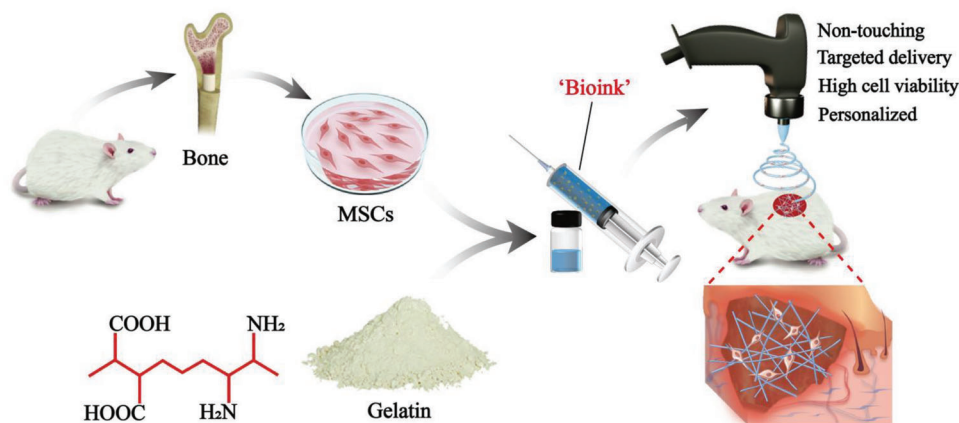


Figure 1. Schematic illustration of in situ cell electrospinning as an attractive stem cell delivery approach for cutaneous wound healing.

viability of 91.5%, whereas cell electrospay with PBS only exhibited a cell viability of 81.0%. This observation could be attributed to the presence of gelatin polymer within the electrospinning solution. On one hand, gelatin polymer protects cells by increasing the resistance of electrospinning solution.^[21] On the other hand, integrin, an electric field-sensing protein located on the cell surface, could be blocked by gelatin, further protecting the cells from high-voltage damage.^[22,23] Cell delivery through cell spray instruments has been investigated in tissue engineering and regenerative medicine^[11]; cells sprayed by these instruments have shown 47.0–73.3% survival, lower than cell electrospinning in the present study.

2.2. Cell Distribution on Fibers

To visualize the presence of intact MSCs within the fibers, MSCs that were transfected with a green fluorescent protein (GFP) adenovirus were employed for cell electrospinning. It should be noted that GFP-labeled MSCs were only used for visualization and not for other experimental assays, including flow cytometry to prevent any potential interference with the analysis. Figure 2E,F and Figure S4 (Supporting Information) clearly show a homogeneous distribution of MSCs throughout the fabricated structure. Therefore, the cell homogeneity of the spinning solution is maintained during the electrospinning process.

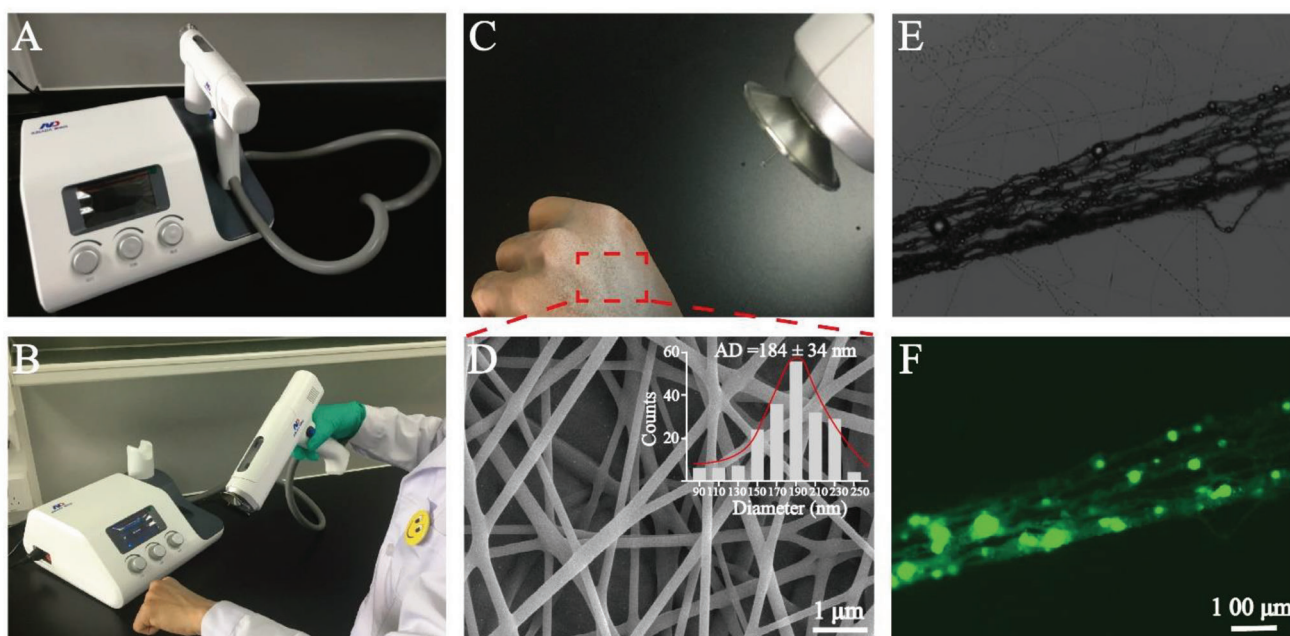


Figure 2. In situ cell electrospinning via a portable electrospinning device. A) The portable electrospinning device used in the present study. B,C) Direct deposition fibers over a hand for 30 s. D) SEM image and fiber diameter distribution highlighted in the red box of (C). E,F) Representative images (E: bright field, and F: fluorescence) of electrospun fibers carrying with living MSCs. MSCs were labeled with GFP.

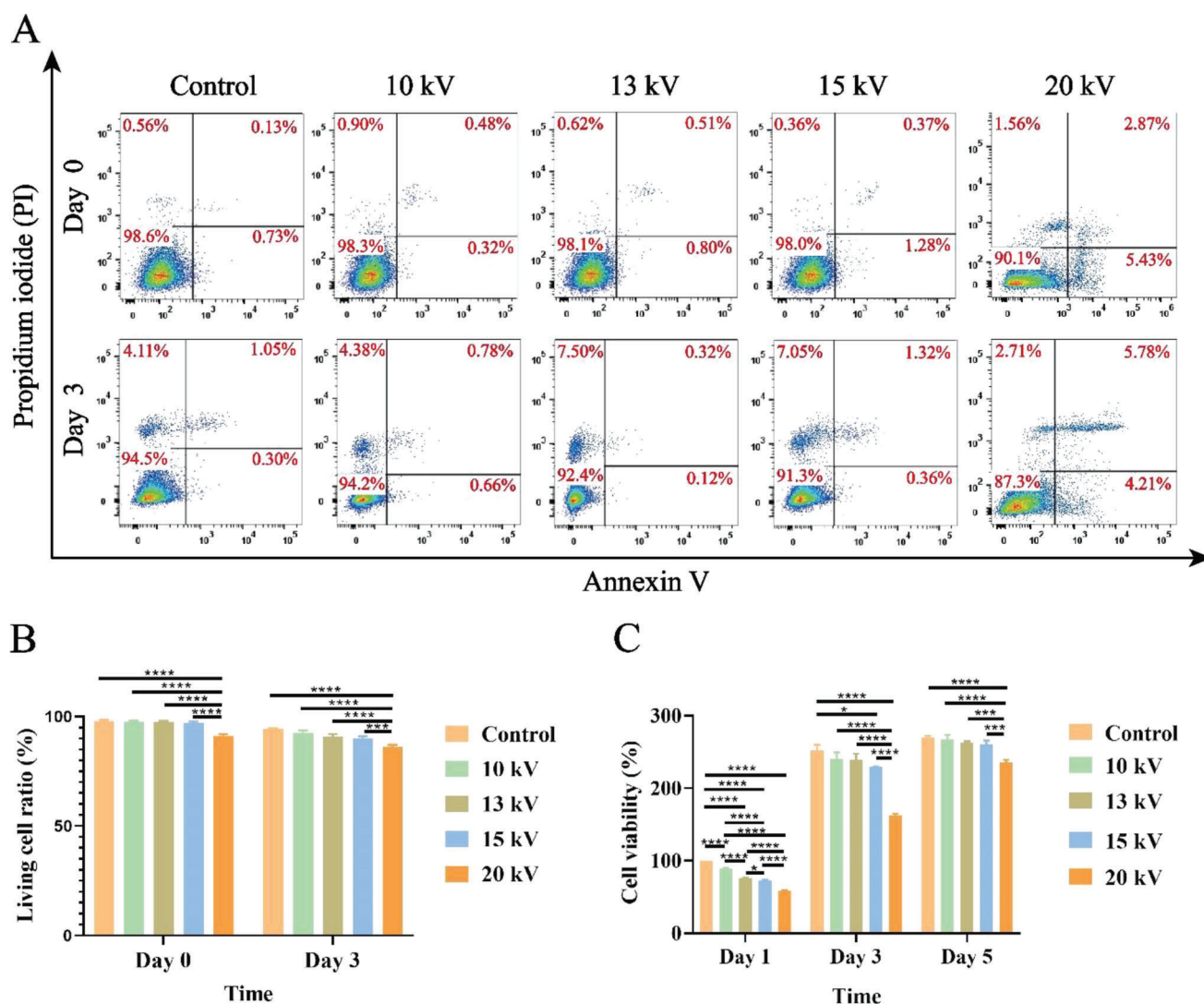


Figure 3. The effect of applied voltage on cell viability. A) Analysis of Annexin V and PI-positive cells by flow cytometry immediately after cell electrospinning and 3 days after electrospinning. Representative scatter plots showing early apoptotic (EA), and apoptotic plus necrotic cell population (N&A) measured as percentages of total gated cells. B) Cell populations represented as percentages of total gated cells, $n = 4$. C) MSC metabolic activity assessed by the CCK-8 assay 1, 3, and 5 days after cell electrospinning, $n = 3$. * $p < 0.05$, *** $p < 0.001$, **** $p < 0.0001$.

2.3. Effect of Applied Voltages on Cell Electrospinning

Electrospinning is characterized by applying a high voltage, which may be deleterious to cellular viability. To assess the effect of applied voltages on cell viability, the applied voltages were varied from 0 to 20 kV while the tip-to-collector distance was kept constant at 5 cm. As shown in Figure S5 (Supporting Information), no significant change in cell morphology was observed regardless of the applied voltage. Cells were further labeled with Annexin V/PI (Propidium Iodide) and detected by flow cytometry immediately after cell electrospinning and 3 days later. As shown in Figure 3A,B, when the applied voltages increased from 0 to 15 kV (the corresponding electric field from 0 to 3 kV mm⁻¹), no significant differences in viable cells were observed post-cell electrospinning at day 0. As the applied voltage increased to 20 kV

(the corresponding electric field of 5 kV mm⁻¹), viable cells decreased significantly to 90.1% at day 0, with the highest level of early apoptosis (5.43%). A similar trend in cell survival rates and apoptosis was observed on day 3. Our results were constant with previous findings that strong electric fields may cause low cell viability.^[24,25] Notably, MSCs displayed a high survival rate superior to 90.0% when the application of electric field was below 5 kV mm⁻¹, suggesting that MSCs are more robust and resistant to electric fields than most cell types previously studied including human brain cells, primary neonatal rat cardiomyocytes, and mouse neuroblastoma N2A cells.^[24,26] This finding was further confirmed using MSCs derived from human bone marrow (Figure S6, Supporting Information). For the 10 and 13 kV cases, reasonable cell viability (over 98.1%) was achieved. However, the fibrous structure started to coagulate significantly with an applied

voltage of 10 kV (Figure S7, Supporting Information). In the following study, cell electrospinning was conducted with an applied voltage of 13 kV.

To further determine whether cell electrospinning affected cell behavior over time, their metabolic activity that reflects the number of living cells in the culture, was evaluated by Cell Counting Kit-8 on days 1, 3, and 5 post-cell electrospinning (Figure 3C). Although metabolic activity increased over 5 days in all groups, it was lower in cell electrospinning groups than the control group (MSCs without cell electrospinning treatment were used as a control) on day 1; however, no significant differences were observed between control and cell electrospinning groups on days 3 and day 5.

2.4. Assessment of MSC Surface Markers and Differentiation Potential Post Cell Electrospinning

Next, we sought to understand the effect of the cell electrospinning process on MSC surface marker expression. MSCs were collected post-cell electrospinning, and a set of specific cell surface markers were identified. As shown in Figure 4A, these cells were negative for markers CD45 and CD11b/c, and highly expressed CD29, CD44, and CD90 surface markers. These surface markers are widely recognized as defining characteristics of MSCs. Similar results were displayed when using bone marrow-derived MSCs (Figure S8, Supporting Information). Taken together, these results indicate that the cell electrospinning process does not adversely affect MSC surface marker expression.

The multi-differentiation potential of MSCs is widely recognized as one of their key features.^[27] To investigate whether the cell electrospinning procedure affected the differentiation potential of MSCs, MSCs post-cell electrospinning were differentiated in osteogenic and adipogenic induction medium for 4 weeks and 5 weeks, respectively. MSCs without cell electrospinning were used as a control. Oil Red O and Alizarin Red staining demonstrated that the MSCs harvested from cell electrospinning could differentiate into adipogenic and osteogenic lineages (Figure 4B). Quantification of the positive area rate (Figure 4C) further confirmed that both calcium deposition and lipid droplets formation in cell ESP group are comparable to that in control group (without cell electrospinning treatment), indicating that cell electrospinning process shows no negative impact on MSCs multiple differentiation potential. Taken together, our results suggest that MSCs maintain their original features and multi-differentiation capacity after cell electrospinning. Our findings are in agreement with previous studies that human adipose-derived MSCs and human deciduous tooth pulp-derived MSCs survived and maintained differentiation potential after cell electrospinning.^[28-30] Similarly, a study by González et al. demonstrated no changes in human neural stem cell differentiation potential after cell electrospinning.^[31]

2.5. Cell Electrospinning Accelerated Wound Healing in Rat Models

In previous sections, we established that the cell electrospinning process yields no adverse effects on MSCs in the short term or

long term. Next, to investigate the potential application of in situ cell electrospinning on stem cell delivery for cutaneous wound healing, full-thickness dorsal wounds were created in rat models. Bioinks were freshly prepared by adding a high-density MSC suspension (10^7 cells in 200 μ L media) into 1 mL cold-water fish gelatin aqueous solution, and then loaded onto a handheld electrospinning apparatus. Therapeutic treatments for wound healing in rats involved the direct deposition of MSC-laden gelatin nanofibers (with the fiber thickness $\approx 300 \pm 20$ μ m) onto the wound sites. As shown in Figure S9 (Supporting Information), the electrospun fibers could adhere to the wound site and match the wound shape properly. It is important to note that the gelatin fibers were not further crosslinked, as their purpose was solely to serve as a carrier for cell delivery and would naturally dissipate within approximately 40 minutes within the wound due to the wet wound environment (Figure S10, Supporting Information). For comparative purposes, three other groups were simultaneously conducted: treatment with a commercial spray gel (3M), fish gelatin nanofibers (Gelatin), and a saline treatment (control). Figure 5A,B shows the representative gross examination of wound images at different time points. The wounds treated with Gelatin and MSCs/Gelatin healed much faster in the early stages of healing (days 3 and 7) and were principally covered with newly formed epidermis at day 14. These observations demonstrated that fish gelatin could promote wound healing while the addition of MSCs yielded a synergistic effect. To measure the speed of wound healing, the wound area was calculated (Figure 5C). It was found that the wound healing rates on days 3, 7, and 14 were considerably faster in the MSCs/Gelatin group when compared with the control group. No significant difference in wound closure was observed on days 21 and 28, irrespective of the treatment provided.

2.6. Histological Analysis of Wounds

The healing pathology of wounds was evaluated by hematoxylin and eosin (H&E) staining (Figure 6A). By day 14, MSCs/Gelatin and Gelatin groups showed substantial granulation tissue with neo-epidermis formation, whereas less regenerated tissue and delayed re-epithelialization were observed in 3M and control groups. By day 28, all wounds were covered with neo-epidermis. However, compared with the MSCs/Gelatin group, the other treatment groups exhibited significantly thicker epidermal layers, exceeding the typical thickness commonly observed in scarred or diseased tissue.^[32] This observation was confirmed by quantification analysis (Figure 6C), showing that the thickness of the epidermis in the MSCs/Gelatin group was comparable to native skin unlike other groups, indicating reduced scarring formation by MSCs. Consistently, studies have shown that MSCs could reduce scarring by regulating inflammation.^[33]

Collagen deposition is one of the key indicators used to characterize the wound healing process.^[34,35] MSCs can activate collagen and elastin deposition by fibroblasts. We conducted Masson trichrome staining to understand whether in situ electrospinning of MSCs/Gelatin could promote collagen deposition and remodeling in wounds. As shown in Figure 6B,D by day 14, collagen deposition in wounds treated with MSCs/Gelatin

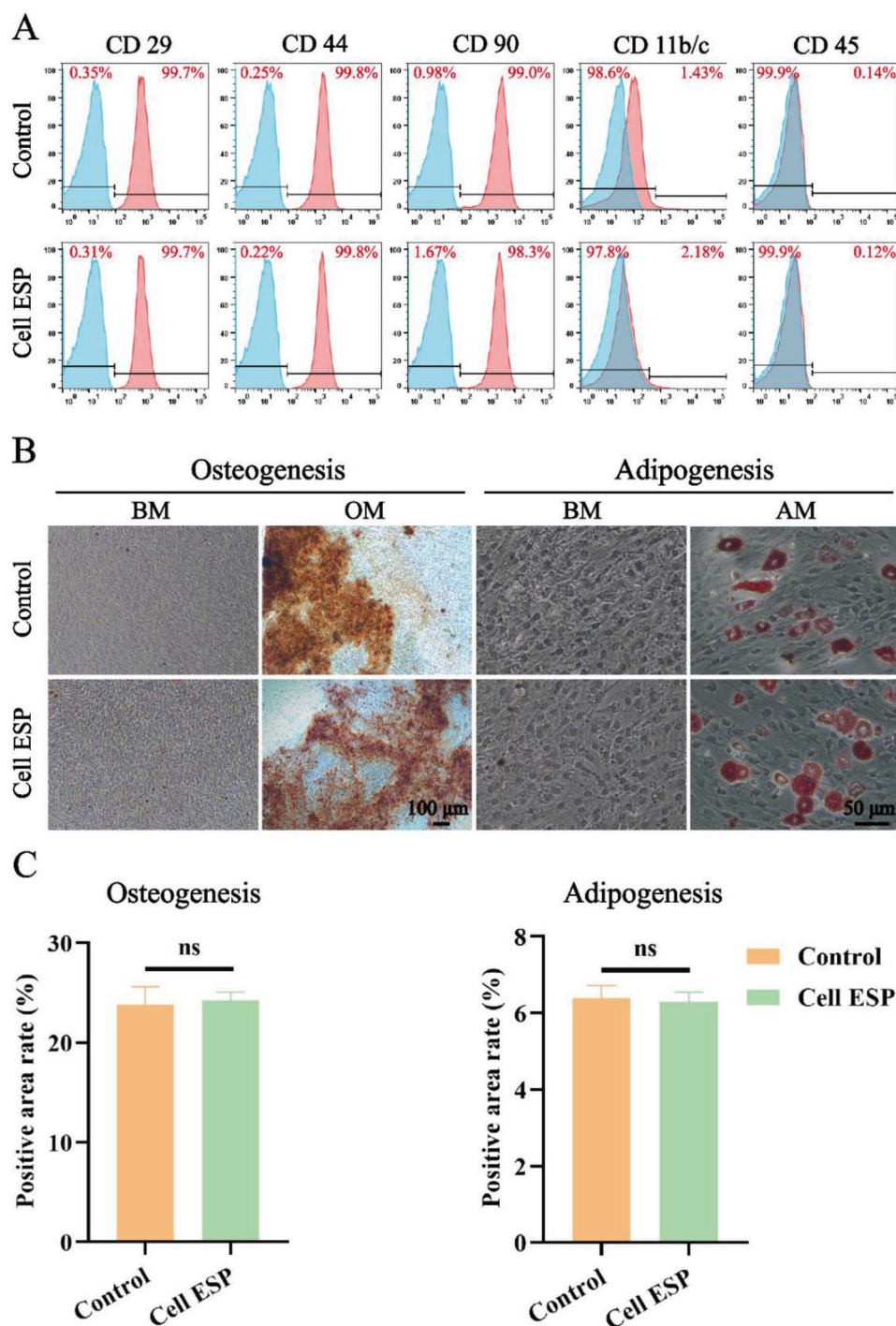


Figure 4. The effect of cell electrospinning process on MSC surface marker expression and differentiation potential. A) Comparative analysis of the expression of MSC-related markers between cell electrospinning group and control group. B) Comparison of MSCs differentiation potential between cell electrospinning groups and control group. C) Quantification of positive area rate of cell mineralization (Left) and lipids formation (Right). $n = 3$. ns: no significance.

was more extensive and evenly distributed in the dermis area throughout the section compared with other conditions. By day 28, the difference was more prominent, as evidenced by the presence of thicker and more mature collagen bundles in MSCs/Gelatin conditions compared to other conditions.

2.7. Enhancement of the Expressions of VEGF/CD31

Revascularization of damaged tissue is essential for wound healing. Indeed, dysregulated or insufficient vessel growth can delay or lead to pathological healing in wounds.^[36] It has been

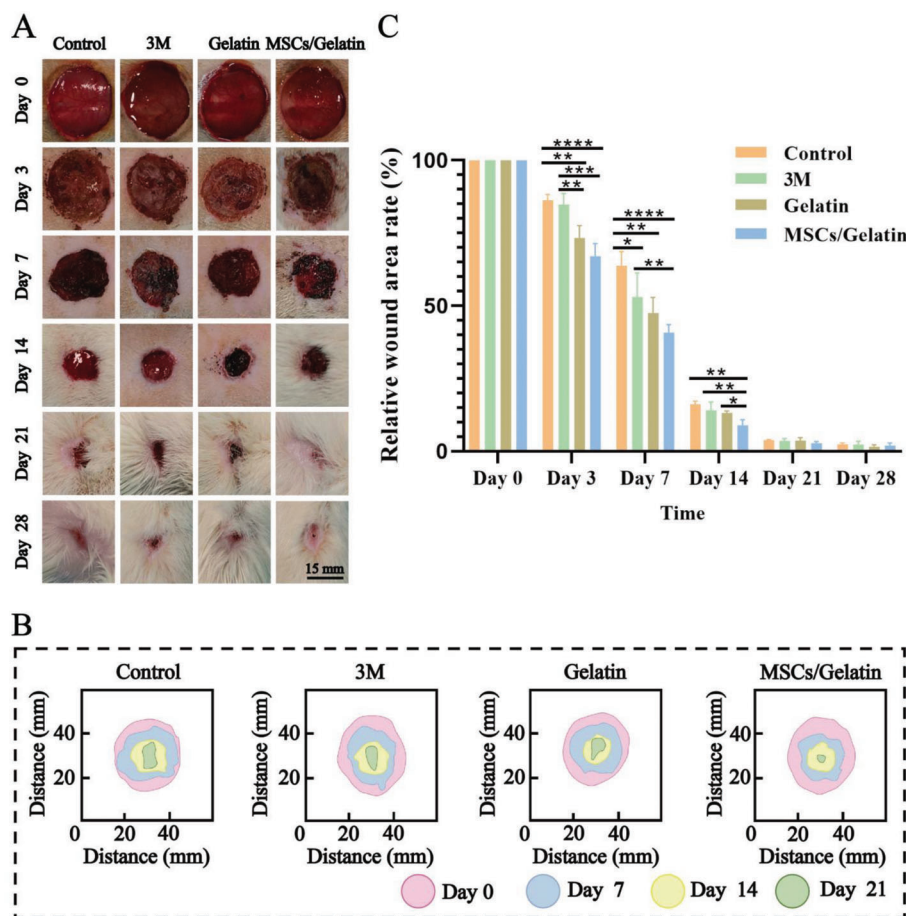


Figure 5. The application of in situ cell electrospinning for cutaneous wound healing. A) Gross observation of wound healing process during 28 days. B) The simulated changes of wound size and morphology during 21 days. C) Statistics of wound closure rates in different groups, $n = 4$. * $p < 0.05$, ** $p < 0.01$, *** $p < 0.001$, **** $p < 0.0001$.

shown that MSCs can accelerate cutaneous wound healing by stimulating angiogenesis.^[37] We conducted immunohistochemistry staining for VEGF to examine whether in situ electrospinning of MSCs/Gelatin could promote angiogenesis in wounds, we conducted immunohistochemistry staining for VEGF. VEGF is a widely acknowledged proangiogenic growth factor in the skin, and regulating VEGF expression in a wound can considerably affect the healing process and outcomes.^[36] As shown in **Figure 7**, on day 14, increased VEGF secretion was observed in MSCs/Gelatin group compared to Control group. Quantitative statistics further confirmed that the abundance of VEGF in MSCs/Gelatin groups was significantly higher than in both 3M and control groups. Immunofluorescence staining for CD31 revealed the significant generation of small blood vessels in all treated groups on day 28. On the other hand, the control group showed a lack of blood vessels due to delayed development of granulation tissue.

2.8. Reduction of IL-6 Expression

Excessive inflammation caused by an infection can reportedly disrupt the wound-healing process. IL-6 is an inflammatory

factor, widely believed to play crucial roles in wound healing by regulating immune response, angiogenesis, and collagen accumulation.^[38] The ability of MSCs to modulate the inflammatory microenvironment and to enhance wound repair has been well characterized.^[39] To know whether in situ electrospinning of MSCs/Gelatin would give rise to better resolution of wound inflammation, we determined the expression of IL-6 in granulation tissues by immunohistochemical staining (**Figure 8**). IL-6 was observed in all groups in the early stage of wound healing (day 3) because of inflammatory response. However, a reduction in inflammatory factor in MSCs/Gelatin and Gelatin groups was observed compared to the untreated groups. On day 14, this phenomenon was more pronounced with a lower abundance of IL-6 in MSCs/Gelatin and Gelatin groups.

Based on our findings obtained from in vivo studies, the in situ cell electrospinning of MSCs/Gelatin exhibited several beneficial effects during the wound healing process, such as reduced scar formation, enhanced neovascularization, and a reduced inflammatory response. These results suggest that MSCs maintain their functions and behaviors even after undergoing in situ cell electrospinning. Although electrospun scaffolds have been broadly investigated for cutaneous wound healing, this approach has limitations, such as using toxic solvents for scaffold fabrication,

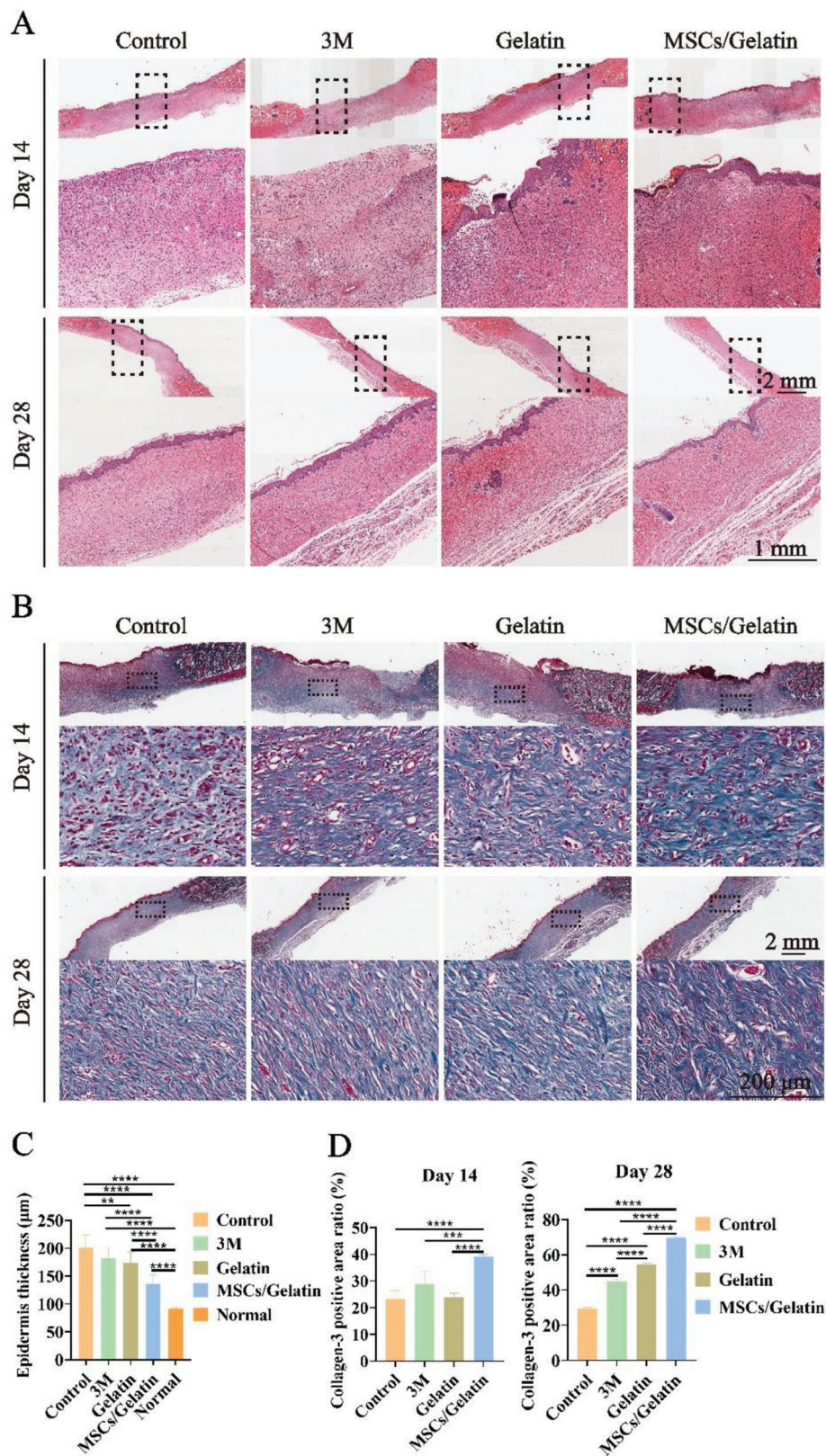


Figure 6. Histological analysis of wound regeneration. A) Representative H&E staining images on days 14 and 28. (B) Representative Masson staining images on days 14 and 28. (C) Quantification evaluation of epidermis thickness based on H&E staining (A), $n = 3$. (D) Quantification of collagen amount in different groups of Masson staining, $n = 3$. $**p < 0.01$, $***p < 0.001$, $****p < 0.0001$.

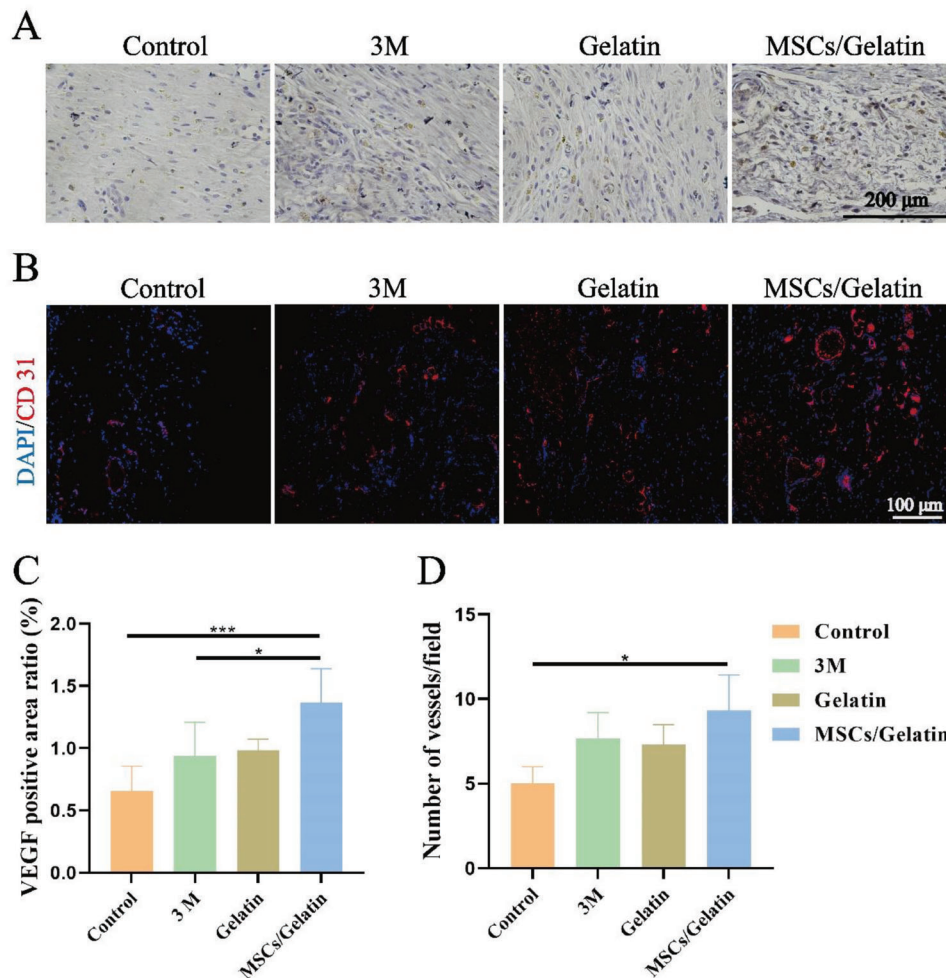


Figure 7. Analysis of new blood vessels formation in wound tissues. A) Representative immunohistochemical staining images of VEGF of wound tissues for different treatments. B) Representative immunofluorescent staining images of CD31 of wound tissues for different treatments. C) Quantification analysis of VEGF expression based on immunohistochemical staining images of VEGF (A), $n = 3$. D) Quantification analysis of vessels number, $n = 3$. * $p < 0.05$, *** $p < 0.001$.

poor cell infiltration, and inhomogeneous cell-distribution.^[40] In contrast, our in situ cell electrospinning approach uses no toxic solvents and works in a single-step manner, which could directly deposit stem cells together with bioactive polymer fibers to wounded sites. Cell electrospinning was first introduced by Jayasinghe et al. in 2006, and this concept was then extended by exploiting various types of biomaterials, including polyvinyl alcohol (PVA), alginate, poly(dimethylsiloxane), polyethylene oxide (PEO), and Matrigel.^[24] In addition, cell electrospinning has been applied for various applications in regenerative medicine, such as skeletal muscle regeneration,^[24] bone tissue engineering,^[25] and heart tissue engineering.^[41] However, few studies on in situ cell electrospinning have been conducted. Recently, in situ deposition of PVA/BMSCs (Bone Marrow Mesenchymal Stem cells) fibers onto rat skin wounds has been investigated using a handheld electrospinning apparatus.^[42] To our knowledge, this is the first report that cold-water fish gelatin is a promising biomaterial for cell electrospinning. The cold-water fish gelatin is a cell-friendly biomaterial with excellent spinnability at room or human temperature. In contrast with previous investigations, the surface

markers of MSCs were monitored post-cell electrospinning in the present study.^[22,42] Taken together, our findings based on in vitro and in vivo studies provide compelling evidence that in situ cell electrospinning is an effective MSC delivery approach for cutaneous wound healing.

3. Conclusion

In the present work, we successfully demonstrated the proof of concept that in situ cell electrospinning is an attractive stem cell delivery approach for cutaneous wound healing. Analysis of cell viability, surface markers, and differentiation capacity demonstrated that the cell electrospinning process yields no adverse effects on MSCs in the short or long term. Based on this approach, bioactive polymer fibers embedded with living MSCs could be directly deposited onto the wounded skin of rats, leading to an accelerated wound-healing process and less scar formation. Our work opens new avenues for stem cell delivery in regenerative medicine as this novel approach may be similarly useful in treating wounds in other tissues such as muscles.

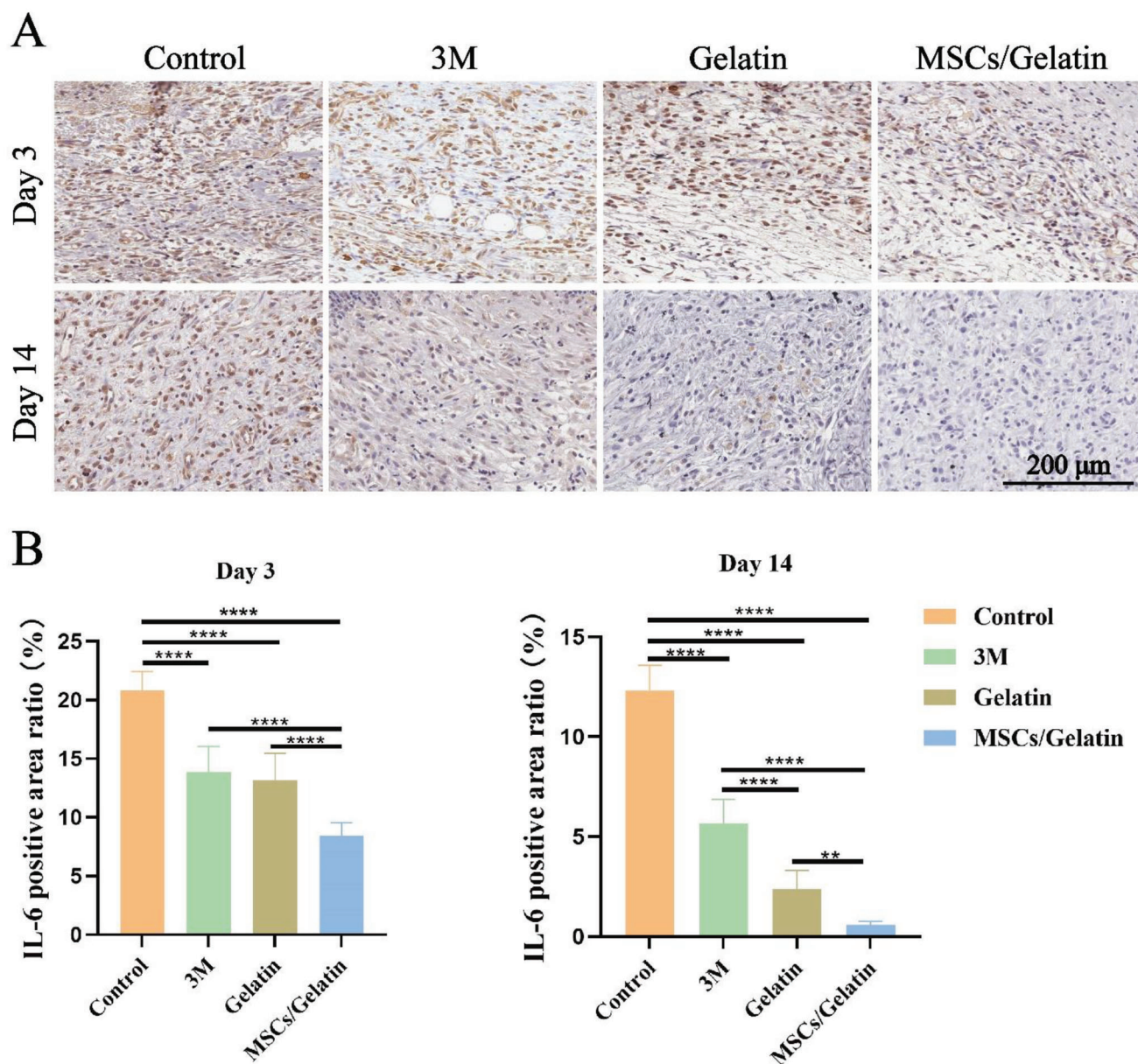


Figure 8. Characterization of inflammatory factor in wound tissues for different treatment. A) Representative images of immunohistochemical staining of interleukin (IL)-6 on days 3 and 14. B) Quantification analysis of IL-6 based on immunohistochemical staining images (A), $n = 3$. $**p < 0.01$, $****p < 0.0001$.

4. Experimental Section

Cell Culture: Sprague–Dawley rat bone marrow-derived mesenchymal stem cells and human bone marrow-derived mesenchymal stem cells were purchased from Cyagen, China. MSCs were cultured in basic medium (BM), comprising a Minimum Essential Medium- α (MEM- α , Gibco), 10% fetal bovine serum (FBS, Vistech), 2 mM GlutaMAX (Gibco), 100 U mL⁻¹ penicillin, and 100 mg mL⁻¹ streptomycin (Gibco) and incubated at 37 °C in a humidified atmosphere of 5% CO₂. The culture medium was changed every 3 days. Cells were harvested at $\approx 90\%$ confluence for further bioink preparation.

Preparation of Gelatin Solution and Bioink: Gelatin from cold-water fish skin (Type A, 300 bloom, average MW = 50 000–100 000 Da,

Sigma) was first sterilized by autoclaving, and then dissolved in sterile phosphate-buffered saline (PBS, 1 \times , pH 7.4) with a final concentration of 50% (w/v). The solution was stirred using a magnetic bar at room temperature overnight. As a bioink, 1×10^7 MSCs were suspended in 200 μ L PBS, then added into 1 mL gelatin solution and mixed homogeneously.

Cell Electrospinning: The prepared bioink was loaded into a 5-mL sterile disposable syringe (BD Biosciences), to which a 23-gauge blunt-tip needle was connected. Next, the syringe was placed into a portable electrospinning instrument (TTE-1, JUNADA, China) for cell electrospinning. The electrospinning parameters used: the applied voltage = 8–20 kV, flow speed = 40 μ L min⁻¹, and tip-to-collector distance keeping within 5–10 cm. The living electrospun scaffolds were deposited on a cover

glass and observed using a microscope system with a brightfield and fluorescent channels (Axio Imager A2, ZEISS).

Identification of MSCs Surface Markers: The living electrospun scaffolds were deposited into a Petri dish with basic medium. Next, the Petri dish was placed in a 37 °C, 5% CO₂ incubator for 24 h. The next day, MSCs were detached from the Petri dish and were labeled with anti-rat CD 11b/c (Biolegend, 201807, PE), anti-rat CD45 (Biolegend, 202225, Pacific Blue), anti-mouse/rat CD 29 (Biolegend, 102205, FITC), anti-rat CD 90 (Biolegend, 206105, FITC), and anti-rat CD 44H (Biolegend, 203906, FITC). The markers on the cell surface were identified using flow cytometry (FACS Celesta, BD).

Cellular Apoptosis and Viability of MSCs: Electrospun fibers with living cells were collected using a Petri dish that contained MEM- α (10% FBS, 1% penicillin/streptomycin, 1% L-glutamine). Electrospun cells were then centrifuged and collected for apoptosis tests. Cell apoptosis was detected with FITC Annexin V/Dead Cell Apoptosis Kit (Invitrogen) with flow cytometry on days 0 and 3 of culture. Cells were stained with the kit components and incubated at room temperature in the dark for 15 min. Then, the cells filtered through a 70- μ m cell strainer to obtain a single cell suspension and analyzed using flow cytometry (FACS Celesta, BD). For cell proliferation evaluation, electrospun cells were stained by using Cell Counting Kit-8 assay (Sigma–Aldrich) according to the manufacturer's specifications. Briefly, electrospun cells were collected with a 10 cm diameter culture dish containing cell culture medium. The cells were centrifuged and then resuspended in fresh culture medium. They were then seeded in 96-well plates at a density of 2×10^3 cells per well and incubated in a 5% incubator at 37 °C for 1, 3, and 5 days. The absorbances were measured using a multi-function microporous detection plate analysis system (Cytation 5, BioTek) at 450 nm. For both apoptosis tests and cell proliferation evaluations, cells without electrospinning treatments were used as a control.

Comparison of Cell Electrospinning with Gelatin and Cell Electrospinning without Gelatin: For cell electrospinning, the bioink preparation is referred to in Preparation of Gelatin Solution and Bioink. The bioink was prepared for cell electrospinning by suspending 1×10^7 MSCs in 1.2 mL PBS without gelatin, and mixed homogeneously. The parameters for cell electrospinning and cell electrospinning were the same: voltage = 20 kV, flow speed = 40 μ L min⁻¹, and tip-to-collector distance keeping within 5–10 cm. Electrospun or electrospayed cells were collected with a dish that contained MEM- α (10% FBS, 1% penicillin/streptomycin, 1% L-glutamine) and cultured. Cell apoptosis was evaluated at 0, 72, and 120 h of culture. The cells were stained with FITC Annexin V/Dead Cell Apoptosis Kit and incubated at room temperature in the dark for 15 min. Then the cells were passed through a cell strainer of 70- μ m to generate a single cell suspension and analyzed using flow cytometry (FACS Celesta, BD).

The Effect of the Cell Electrospinning Process on the Differentiation Potential of MSCs: During cell electrospinning, electrospun fibers with living cells were collected for 15 min using a Petri dish topped with 10 mL BM. MSC suspension was transferred to Falcon 50 mL conical centrifuge tubes, and centrifuged at 1000 rpm for 5 min at 4 °C. After removing the supernatant, MSC aggregates were resuspended in BM to form a single-cell suspension. MSCs were seeded in 12-well plates at a cell density of 3×10^4 cells per well, and cultured in BM for 3 days.

For osteogenic differentiation, BM was replaced with osteogenic medium (OM) when MSCs reached 80% confluence. Osteogenic differentiation of MSCs was induced by culturing them in OM, which consisted of BM fortified with 10 nm dexamethasone (Sigma–Aldrich), 10 mm β -glycerophosphate (Sigma) and 0.2 mm ascorbic acid (Sigma). The cell culture medium was refreshed every 2 days. After 28 days of culture, the cells were washed with PBS, fixed with 10% formalin for 1 h, and then washed again with PBS and twice with distilled water. The cells were treated with a freshly filtered 2% aqueous alizarin red S solution (pH 4.2) for 5 min. Next, the excess solution was removed by washing the cells with distilled water. Samples were observed by an inverted optical microscope (MODEL ECLIPSE Ts2, Nikon, Japan).

For adipogenic differentiation, BM was replaced with adipogenic medium (AM) when MSCs reached 100% confluence. AM composed of Dulbecco's Modified Eagle Medium (DMEM, high-glucose, Gibco), 10% FBS (fetal bovine serum, Vistech), 1% 2 mm L-glutamine (Gibco), 1% peni-

cillin (100 units mL⁻¹)/streptomycin (100 μ g mL⁻¹) (Gibco), 0.2 mm indomethacin (Sigma), 0.5 mm 3-isobutyl-1-methylxanthine (IBMX, Sigma), 1 μ m dexamethasone (Sigma), and 10 μ g mL⁻¹ insulin (Sigma) were used to induce the adipogenic differentiation of MSCs. Cells were cultured with AM medium for three days, and then replaced with BM for 2 days of culture. After that, cells were treated with AM for 3 days. These processes were repeated 3–5 times. After 28 days of culture, cells were rinsed with PBS twice, fixed with 10% formalin for 2 h, washed with PBS, and stained with 0.5% Oil Red O (Sigma Aldrich) for 5 min. The excess Oil Red O solution was washed off with PBS, and then samples were observed by an inverted optical microscope (MODEL ECLIPSE Ts2, Nikon, Japan).

Full-Thickness Wound Healing: All animal experiments were conducted in compliance with Chinese laws and policies after obtaining the approval of the Ethical Committee of the South China University of Technology (AEC: #2020060). SD rats (7 weeks old) were purchased from Hunan SJA Laboratory Animal Co., Ltd (Changsha, China). All rats were housed in a controlled environment with a temperature of 25 ± 1 °C, a relative humidity of 60%, and a 12 h light/dark cycle. All rats were provided with free access to food and water.

Forty SD rats were randomly divided into four groups for the study. Under anesthesia, a full-thickness skin injury measuring 3 cm in diameter was created on the backs of the rats. Group A served as the control group and received no treatment, group B rats were treated with a commercial trauma spray gel (3M, USA), group C rats were treated with gelatin fibers by 12 min in situ electrospinning for each wound, and group D rats were treated with MSCs/Gelatin fibers by 12 min in situ electrospinning for each wound. The treatments were administered only once on Day 0. Gross photographs of the wound areas were captured to visualize the changes in wound size. The wound area was obtained by using Image J software, and wound healing rates were calculated according to the formula: open wound area rates (%) = $(A_t/A_0) \times 100\%$, where A_0 is the initial wound area, A_t is the wound area on Day t .

Histological Analysis: The tissue samples were fixed overnight in 10% neutral buffered formalin at 4 °C, washed with PBS, dehydrated through a graded ethanol series, infiltrated with liquid paraffin overnight, and embedded in paraffin. Sections that were 5–7 μ m thick were cut with a microtome (HM355S, Thermo Fisher Scientific), mounted on poly-lysine precoated slides, and stained with hematoxylin and eosin (H&E) and Masson's trichrome. Microphotographs were then acquired using a microscope (Nikon Eclipse Ti-S) equipped with a color camera (MSX2, Nikon). Quantitative analysis of collagen was conducted by using Image J software.

Immunohistochemical Staining: The tissue samples were fixed in 4% paraformaldehyde at 4 °C for 24 h, dehydrated with gradient alcohol, and embedded in paraffin. First, the samples were heated with microwave in citrate buffer for 15 min. Second, the tissues were blocked with goat serum at room temperature for 1 h. Then incubated with primary antibodies for interleukin-6, (IL-6, Novus, 1:100) and vascular endothelial growth factors (VEGF, Novus, 1:100) at 4 °C overnight, respectively. Third, the tissues were washed with PBS three times, incubated with a diaminobenzidine (DAB) color rendering kit (CWBI) at room temperature for 30 min, rinsed with PBS three times, and a color rendering solution was added. After 5 min, rinsed with PBS, the nucleus was stained with sumousin for 10 min, and cleaned with running water. Finally, a gradient alcohol and xylene dehydration process was carried out, followed by sealing with neutral resin. The tissues were scanned using a pathological scanner (Aperio CS2).

Immunofluorescence Staining: The tissue samples were fixed in 4% paraformaldehyde for 30 min, permeabilized with 0.5% Triton-X in PBS for 10 min, blocked in goat serum (Boster Biological Technology) at room temperature for 1 h, and stained with primary antibody anti-rabbit CD31 polyclonal antibody (1:100, ReliaTech GmbH) at 4 °C overnight. Then tissue samples were washed three times with PBS, and incubated with the secondary antibody of anti-mouse IgG Alexa Fluor 594 (1:1000, Cell Signaling Technology) at room temperature for 2 h. The nucleus was stained with 4',6-diamidino-2-phenylindole (DAPI). Immunofluorescence images were taken by using a Nikon Ti-E A1 confocal laser-scanning microscope (Nikon).

Statistical Analysis: All data were analyzed using a GraphPad Prism 9 software (9.0 version, GraphPad). The number of replicates and samples were shown in the figure legends in each case and the results were presented as mean±standard deviation. One-way ANOVA assessed the differences between groups, followed by Tukey's multiple comparison post hoc test. A probability value of less than 0.05 was considered significantly different (* $p \leq 0.05$, ** $p \leq 0.01$, *** $p \leq 0.001$, and **** $p \leq 0.0001$).

Supporting Information

Supporting Information is available from the Wiley Online Library or from the author.

Acknowledgements

This work was supported in part by the National Natural Science Foundation of China (No. 32071360 and No. 31900976), by the National Key Research and Development Program of China (2018YFA0108200), Research Starting Funding of South China University of Technology (D6181910, D6201880, K5180910, and K5204120), by Research Agreement between South China University of Technology and Guangzhou First People's Hospital (D9194290 and PT31900976). The Guangdong Province Basic and Applied Basic Research Foundation (No. 2021A1515110236), the Science and Technology Program of Guangzhou (No. 202201010248), the Youth Innovation Project of Guangdong Education Department (2020KQNCX018), and the Young Scholar Foundation of South China Normal University (21KJ08).

Conflict of Interest

The authors declare no conflict of interest.

Author Contributions

Z.W. was associated with methodology, investigation, visualization, formal analysis, and wrote the original draft. Y.C. contributed to methodology, investigation, and visualization. P.L., F.W., W.Z., S.L., H.W., and N.W. performed investigations. L.M. reviewed and edited the final manuscript. M.Z. and Y.D. supervised the study, acquired resources, reviewed and edited the final manuscript, and acquired funding. H.C. was associated with conceptualization, supervision, resources, wrote the original draft, reviewed and edited the final manuscript, and acquired funding.

Data Availability Statement

The data that support the findings of this study are available from the corresponding author upon reasonable request.

Keywords

cell electrospinning, gelatin, in situ tissue regeneration, mesenchymal stem cells, portable electrospinning, skin wound healing

Received: March 27, 2023
Revised: June 10, 2023
Published online: July 9, 2023

[1] A. N. Dehkordi, F. M. Babaheydari, M. Chehelgerdi, S. R. Dehkordi, *Stem Cell Research & Therapy* **2019**, *10*, 111.

- [2] H. Sorg, D. J. Tilkorn, S. Hager, J. Hauser, U. Mirastschijski, *Eur. Surgical Res.* **2017**, *58*, 81.
- [3] M. Sheikholeslam, M. E. E. Wright, M. G. Jeschke, S. Amini-Nik, *Adv. Healthcare Mater.* **2018**, *7*, 1700897.
- [4] X. B. Fu, *Int. J. Burns Trauma* **2020**, *8*, tkaa038.
- [5] E. M. Tottoli, R. Dorati, I. Genta, E. Chiesa, S. Pisani, B. Conti, *Pharmaceutics* **2020**, *12*, 735.
- [6] S. Maxson, E. A. Lopez, D. Yoo, A. Danilkovitch-Miagkova, M. A. Leroux, *Stem Cells Transl. Med.* **2012**, *1*, 142.
- [7] L. Y. Peng, Z. Q. Jia, X. H. Yin, X. Zhang, Y. A. Liu, P. Chen, K. T. Ma, C. Y. Zhou, *Stem Cells Dev.* **2008**, *17*, 761.
- [8] D. E. Lee, N. Ayoub, D. K. Agrawal, *Stem Cell Res. Ther.* **2016**, *7*, 37.
- [9] M. Isakson, C. de Blacam, D. Whelan, A. McArdle, A. J. P. Clover, *Stem Cells Int* **2015**, *2015*, 831095.
- [10] K. McFarlin, X. Gao, Y. B. Liu, D. S. Dulchavsky, D. Kwon, A. S. Arbab, M. Bansal, Y. Li, M. Chopp, S. A. Dulchavsky, S. C. Gautam, *Wound Repair Regen* **2006**, *14*, 471.
- [11] S. Motamedi, A. Esfandpour, A. Babajani, E. Jamshidi, S. Bahrami, H. Niknejad, *Tissue Engg. Part C-Me* **2021**, *27*, 543.
- [12] F. Shojaei, S. Rahmati, M. B. Dehkordi, *Wound Repair Regen* **2019**, *27*, 661.
- [13] K. Siimon, P. Reemann, A. Poder, M. Pook, T. Kangur, K. Kingo, V. Jaks, U. Maeorg, M. Jarvekulg, *Mat Sci Eng C-Mater* **2014**, *42*, 538.
- [14] H. W. Kwak, M. Shin, J. Y. Lee, H. Yun, D. W. Song, Y. Yang, B. S. Shin, Y. H. Park, K. H. Lee, *Int. J. Biol. Macromol.* **2017**, *102*, 1092.
- [15] A. H. Grobbs, P. J. Steele, R. A. Somerville, D. M. Taylor, *Biotechnol. Appl. Biochem.* **2004**, *39*, 329.
- [16] A. Dart, M. Bhave, P. Kingshott, *Macromol. Biosci.* **2019**, *19*, 1800488.
- [17] X. Yan, M. Yu, S. Ramakrishna, S. J. Russell, Y. Z. Long, *Nanoscale* **2019**, *11*, 19166.
- [18] R. H. Dong, Y. Li, M. A. Chen, P. H. Xiao, Y. F. Wu, K. Zhou, Z. Zhao, B. Z. Tang, *Small Methods* **2022**, *6*, 2101247.
- [19] Y. T. Zhao, J. Zhang, Y. Gao, X. F. Liu, J. J. Liu, X. X. Wang, H. F. Xiang, Y. Z. Long, *J. Nanobiotechnol.* **2020**, *18*, 111.
- [20] M. Yang, S. H. He, Z. Y. Su, Z. H. Yang, X. X. Liang, Y. Z. Wu, *ACS Omega* **2020**, *5*, 21015.
- [21] F. Topuz, T. Uyar, *ACS Omega* **2018**, *3*, 18311.
- [22] N. Nosoudi, A. J. Oommen, S. Stultz, M. Jordan, S. Aldabel, C. Hohne, J. Mosser, B. Archacki, A. Turner, P. Turner, *Bioengineering* **2020**, *7*, 21.
- [23] C. H. Tsai, B. J. Lin, P. H. Chao, *J. Orthop. Res.* **2013**, *31*, 322.
- [24] M. Yeo, G. H. Kim, *Small* **2018**, *14*, 1803491.
- [25] M. Yeo, G. Kim, *Chem. Eng. J.* **2015**, *275*, 27.
- [26] A. Townsend-Nicholson, S. N. Jayasinghe, *Biomacromolecules* **2006**, *7*, 3364.
- [27] A. Madeira, C. L. da Silva, F. dos Santos, E. Camafeita, J. M. S. Cabral, I. Sa-Correia, *PLoS One* **2012**, *7*, 43523.
- [28] C. Ye, Z. X. He, Y. F. Lin, Y. Zhang, J. Tang, B. Sun, M. X. Ma, J. L. Liu, L. Yang, H. X. Ren, B. P. Zhao, *Biotechnol. Lett.* **2015**, *37*, 449.
- [29] D. I. Braghirolli, F. Zamboni, E. A. X. Acasigua, P. Pranke, *Int. J. Nanomed.* **2015**, *10*, 5159.
- [30] D. I. Braghirolli, F. Zamboni, P. C. Chagastelles, D. J. Moura, J. Saffi, J. A. P. Henriques, D. A. Pilger, P. Pranke, *Biomicrofluidics* **2013**, *7*, 044130.
- [31] C. H. Gonzalez, S. N. Jayasinghe, P. Ferretti, *F1000Res* **2020**, *9*, 267.
- [32] C. O. Chantre, P. H. Campbell, H. M. Golecki, A. T. Buganza, A. K. Capulli, L. F. Deravi, S. Dauth, S. P. Sheehy, J. A. Paten, K. Gledhill, Y. S. Doucet, H. E. Abaci, S. Ahn, B. D. Pope, J. W. Ruberti, S. P. Hoerstrup, A. M. Christiano, K. K. Parker, *Biomaterials* **2018**, *166*, 96.
- [33] R. Guillaumat-Prats, *Cells* **2021**, *10*, 1729.
- [34] Y. Xi, J. Ge, M. Wang, M. Chen, W. Niu, W. Cheng, Y. Xue, C. Lin, B. Lei, *ACS Nano* **2020**, *14*, 2904.
- [35] S. S. Mathew-Steiner, S. Roy, C. K. Sen, *Bioengineering* **2021**, *2021*, 8.

- [36] P. Bao, A. Kodra, M. Tomic-Canic, M. S. Golinko, H. P. Ehrlich, H. Brem, *J. Surg. Res.* **2009**, *153*, 347.
- [37] Y. L. Li, L. Zheng, X. Xu, L. L. Song, Y. Li, W. Li, S. H. Zhang, F. Zhang, H. Y. Jin, *Stem Cell Res. Ther.* **2013**, *4*, 113.
- [38] Z. Q. Lin, T. Kondo, Y. Ishida, T. Takayasu, N. Mukaida, *J. Leukocyte Biol.* **2003**, *73*, 713.
- [39] K. C. Murphy, J. Whitehead, D. J. Zhou, S. S. Ho, J. K. Leach, *Acta Biomater.* **2017**, *64*, 176.
- [40] J. Hong, M. Yeo, G. H. Yang, G. Kim, *Int. J. Mol. Sci.* **2019**, *20*, 6208.
- [41] E. Ehler, S. N. Jayasinghe, *Analyst* **2014**, *139*, 4449.
- [42] S. N. Xu, T. Lu, L. Yang, S. W. Luo, Z. Wang, C. Ye, *Int. Wound J.* **2022**, *19*, 1693.